Preparation and Physicochemical Properties of Biochar from the Pyrolysis of Pruning Waste of Typical Fruit Tree in North China

Xuelei Liu,[a] Xueyong Ren,[a,*] Jiangchuan Dong,[a] Bowei Wang,[a] Jianli Gao,[b] Ruijiang Wang,[b] Jingjing Yao,[c] and Wenbo Cao [a,c]

Routine maintenance of fruit trees generates a substantial quantity of pruning waste each year. This waste is potential feedstock for producing energy, materials, and other products. The feasibility of making biochar from the waste *via* pyrolysis was evaluated. The effects of seven tree species, different pruning sites, and temperature on the pyrolysis process, and the physicochemical properties of the biochar were studied. Pyrolysis of different tree species at 500 °C yielded 27.5 to 33.3% biochar, with a high calorific value (approximately 30 MJ/kg), low ash content (approximately 4%), and capturing up to 60% of the carbon element present. Simultaneously, when the temperature was increased from 400 to 700 °C, the yield of biochar decreased from 35.8% to 24.3%, but the properties improved with the higher heating value rising from 29.2 to 31.3 MJ/kg and the iodine value from 234 to 252 mg/g. The biochar has a good pore structure with a specific surface area of 237 m^2/g, total pore volume of 0.175 cm^3/g, and average pore size of 2.96 nm. In general, biochar from the pyrolysis of fruitwood pruning waste generated here could be an ideal feedstock to produce high-value-added products, such as solid fuels, activated carbon, and electrode materials.

DOI: 10.15376/biores.18.4.8536-8556

Keywords: Fruit tree pruning waste; Pyrolysis; Biochar; Pore structure; Physical and chemical properties

*Contact information: a: National Forestry Grassland Wood Material Recycling Engineering Technology Research Center, College of Materials Science and Technology, Beijing Forestry University, Beijing 100083, China; b: Chengde Forestry and Grassland Technology Extension Station, Chengde, 067000, China; c: Institute of Resources and Environment, Beijing Academy of Science and Technology, Beijing, 100095, China; *Corresponding author: rxueyong@bjfu.edu.cn*

INTRODUCTION

Fruit trees, as a commercially important forest type in China, not only generate immense economic value by supplying fruits every year but also absorb carbon dioxide and help to achieve carbon reduction targets. In the daily management of orchards, fruit trees must be pruned to ensure the quality and yield of fruit, which generates a considerable amount of pruning waste worldwide (Brand and Jacinto 2020). If orchards produce an average of 0.5 tons of fruit tree pruning wastes per 667 m^2 per year, then the aggregate number of pruning wastes in China's orchards could potentially reach 97 million tons in 2022. The European Union yields an estimated 25 million tons of wood waste annually (Aliaño-González *et al*. 2022). Pruning waste from fruit trees needs to be treated and utilized properly. Otherwise, the material is susceptible to fire, pests, and diseases, which affect fruit production and reduce the economic benefits of the orchard. Further, such

wastage is also not conducive to reducing carbon emissions. Seibold *et al*. (2021) reported that dead wood worldwide releases 1.09 billion tons of carbon per year, which is 1.15 times the amount of fossil fuel emissions. Therefore, there is an urgent demand for the effective utilization of fruit tree pruning waste.

In fact, pruning waste of fruit trees are a type of lignocellulosic biomass, which is a clean renewable resource rich in organic matter including cellulose, hemicellulose, and lignin. Conventional disposal methods typically involve incineration or landfill, which not only pollute the environment but also result in wasting precious resources. Numerous studies have reported on the potential uses of pruning, such as pyrolysis for the preparation of biochar, cultivation of edible fungi, fermentation for the production of organic fertilizers, manufacture of wood-based panels (Lee *et al*. 2022), and the making of solid biofuel for heating (Soltero *et al*. 2020). Among these, pyrolysis technology deserves attention because of its benefits of strong adaptability to feedstock, high processing capacity, continuous production, and clean and renewable products.

Pyrolysis is a promising technology that enables biomass to be thermally broken down to obtain products such as biochar, bio-oil, and syngas in an oxygen-free, high-temperature environment (300 to 900 °C) (Kan *et al*. 2016). The pruning waste of fruit wood have a high lignification degree and low ash content, which means that it is a good raw material for pyrolytic carbonization. Typically, a higher yield of biochar is obtained with a heating rate of no more than 30 °C/min, a heating temperature between 400 and 800 °C, and a residence time of more than 600 s (Yu *et al*. 2022b). Biochar is one of the main products of pyrolysis and has a high calorific value, high carbon content, well-developed pore structure, abundant surface functional groups, good stability, and durability. It can be used to produce a wide range of high-value-added char materials, such as fuels (Thakkar *et al*. 2016), activated carbon (Januszewicz *et al*. 2020; Cheng *et al*. 2021), carbon-based fertilizers, soil amendments (Li *et al*. 2020), and electrode materials (Cheng *et al*. 2022), which are widely used in the energy, environmental, and agricultural sectors. Therefore, the pyrolysis of fruitwood pruning wastes not only creates additional economic value for the agroforestry industry, but also effectively reduces the amount of carbon dioxide emitted from the natural decomposition of those waste.

Generally, the yield and quality of biochar are affected by pyrolysis factors such as temperature (Lin *et al*. 2022; Agweh *et al*. 2023), feedstock type (Bednik 2022; Burachevskaya *et al*. 2023), heating rate, and residence time. Higher temperatures, lower heating rates, and longer residence times generally help to improve biochar quality (Yang *et al*. 2020). Liu *et al*. (2023) investigated the effects of temperature and type of pecan feedstock (branches, leaves, and nut shells) on biochar. It was found that with the temperature increase, the specific surface area, total pore volume, pH value, and content of certain elements (calcium, magnesium, iron, manganese, and copper) of the three types of biochar showed an upward trend, but the yield apparently decreased. Among them, leaf biochar had the highest yield. Pecan branch and leaf biochar contained more nutrient minerals than nutshell biochar and could be used to improve soil fertility. Chen *et al*. (2016) studied the impact of heating rate and temperature on the pyrolysis products of poplar wood, and it was found that the bio-oil yield was higher at 500 °C with larger heating rate, while higher mass and energy yield of biochar was achieved at lower temperature and heating rate. Increasing the heating rate favored the production of CO and CH_4, which in turn increased the carbon content of the biochar. The residence time also has a significant influence on the structure of biochar (Shaaban *et al*. 2014). The degree of carbonization,

pH, and aliphatic functional groups of the biochar increased with the extension of the residence time.

The potential of fruitwood waste as a valuable resource for the production of biochar remains largely unexploited. In this study, based on the concept of minimizing energy consumption and CO_2 emissions with precisely optimizing the pyrolysis process of typical feedstock, the pyrolysis conditions were studied. The index of energy consumption (electric power) data and carbon yields were used as the evaluation target. The goal here was to correlate the data with the feedstock composition of fruitwood, as well as the properties of final biochar products. Starting from the composition and basic characteristics of fruit tree pruning waste, this study investigated the effects of tree species, temperature, and pruning site on the physicochemical properties of biochar produced by pyrolysis, and studied the effects of different experimental conditions on the energy consumption, product yield, and carbon sequestration. The aim was to provide a viable method of using fruit tree pruning waste and broaden the source of feedstock for biochar production, and then supply a theoretical basis for the optimization of the charring process. Preparation of biochar from fruit tree pruning wastes not only minimizes the environmental burden caused by the feedstock, but it also provides a means of using the fruit wood waste in a resource-efficient manner.

EXPERIMENTAL

Materials

Pruning waste from Hebei and Henan provinces in northern China was collected from the seven different types of fruit trees, namely apricot (*Armeniaca vulgaris Lam*) tree (AT), apricot plum (*Armeniaca mume* var. *bungo* Makino) tree (APT), walnut (*Juglans regia Linn*) tree (WT), chestnut (*Castanea mollissima* Blume) tree (WT), peach (*Prunus persica* (L.) tree (PT), mountain apricot (*Armeniaca sibirica* (Linn.) Lam) tree (MAT), and mountain peach (*Amygdalus davidiana* (Carrière) de Vos ex Henry) tree (MPT). Among them, the main branches (MB) and lateral branches (LB) of mountain apricot and mountain peach trees were clipped from different parts. These raw materials were sourced from fruit trees that were growing vigorously, except for chestnut tree pruning wastes, which were cut from old trees and had a relatively high bark content. This batch of fruit wood was cut to a size of 5 to 6 cm and dried in a ventilated and dry place for several days to reach an air-dried state.

Composition Analysis Methods of Feedstocks

The carbon, hydrogen, and nitrogen content in fruit tree branches were determined using a SDCHN 435 elemental analyzer (SDCHN435 Carbon & Hydrogen & Nitrogen analyzer, Changsha, China). The oxygen content was calculated by subtracting the mass fraction of carbon, hydrogen, nitrogen, and ash from the total mass fraction of the sample (100%). The proximate analysis was performed using a SDTGA industrial analyzer (SDTGA5000a proximate analyzer, Changsha, China). The Extract, Holocellulose, and Klason lignin contents in fruit trees were determined in accordance with Chinese national standards GB/T 2677.6(1994), GB/T 2677.10(1995), and GB/T 2677.8(1994), respectively. The higher heating value (HHV) of different fruit tree branches was determined using an IKA C2000 calorimeter (IKA C2000 Calorimeter, Staufen, Germany).

Pyrolysis Equipment and Procedures

Pyrolysis of fruit tree pruning wastes took place in a carbonization furnace, which was independently self-designed and manufactured. Figure 1 is a schematic diagram of the pyrolysis equipment. The weighed fruit wood pruning was placed in the material frame of the equipment, and then the material frame was placed in the carbonization furnace for pyrolysis. Approximately 4 kg of sample was pyrolyzed at a time under the experimental conditions of 15 ℃/min and 500 ℃. While the peach wood pruning was pyrolyzed at temperatures of 400, 500, 600, and 700 ℃ to analyze the influence of temperature on power consumption, pyrolysis product distribution, and properties of biochar.

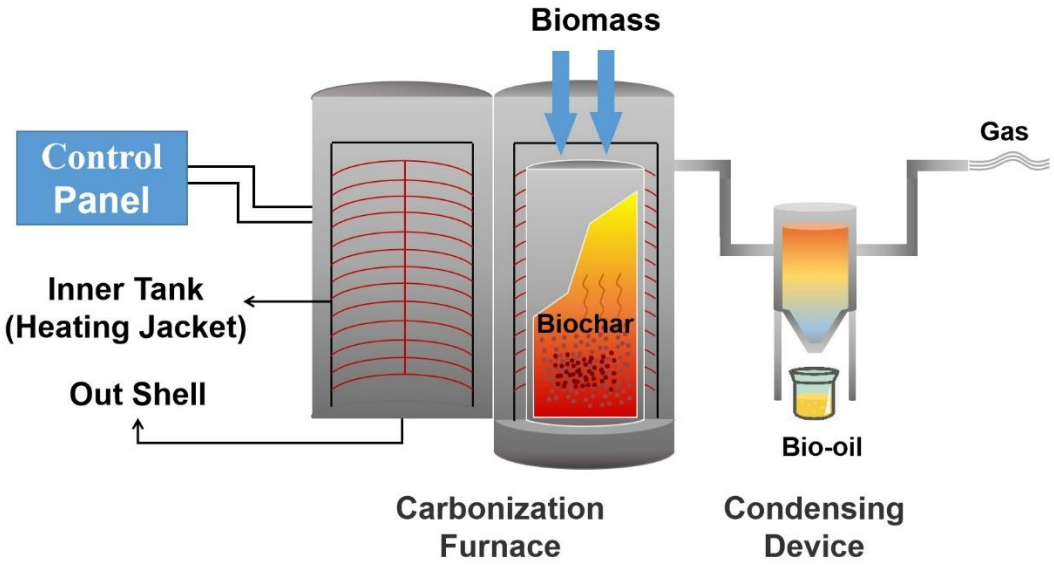

Fig. 1. Schematic diagram of the pyrolysis equipment

Equations

The normal operation of the equipment requires electricity to drive, therefore the amount of electricity consumed during heating and insulation was recorded by the meter.

The yield of biochar (α), the product of pruning pyrolysis of fruit wood, was calculated with Eq. 1,

$$\alpha\,(\%) = \left(W_{\text{biochar}}/W_{\text{feeding material}}\right) \times 100 \quad (1)$$

where W_{biochar} and $W_{\text{feeding material}}$ respectively represent the mass (g) of biochar and feeding material (fruit tree pruning wastes).

The carbon sequestration of biochar was calculated using Eq. 2,

$$\beta = (\alpha \times \emptyset)/\gamma \times 100\% \quad (2)$$

where α, $\emptyset$, and γ respectively indicate the yield of biochar, the carbon content (wt%) of biochar, and carbon content (wt%) in the feedstock.

Properties Analysis Methods of Biochar

Biochar was divided into three categories according to the different pyrolysis tree species, pruning sites, and pyrolysis temperatures. The first type of biochar varied according to the tree species, while other conditions remained the same, including apricot tree biochar (*ATB*), apricot plum tree biochar (*APTB*), walnut tree biochar (*WTB*), and

chestnut tree biochar (*CTB*). The second category was biochar obtained by pyrolysis of different pruning sites (main branches, lateral branches) of the same tree species (mountain apricot tree, mountain peach tree), abbreviated as *MATB-MB*, *MATB-LB*, *MPTB-MB*, and *MATB-LB*, respectively. The third type was the biochar obtained from the same tree species (peach tree) at different pyrolysis temperatures (400, 500, 600, and 700 ℃), named *PTB-400* ℃, *PTB-500* ℃, *PTB-600* ℃, *PTB-700* ℃, respectively. The basic composition, micromorphology, crystalline structure, and pore structure of the biochar were characterized as follows.

Composition analysis methods and calorific value of biochar

The elemental content of carbon, hydrogen, nitrogen, and oxygen in biochar was determined by using the SDCHN 435 elemental analyzer (Changsha, China). The contents of moisture, ash, volatile, and fixed carbon in biochar were determined using a SDTGA 5000a industrial analyzer (Changsha, China). The working temperature of each index of the industrial analyzer was 105 ℃ for moisture, 815 ℃ for ash content, and 910 ℃ for volatile matter, respectively. The amount of fixed carbon was calculated by subtracting the amount of water, ash, and volatile matter. The *HHV* of biochar obtained under different experimental conditions was measured using an IKA C2000 calorimeter (IKA C2000 Calorimeter, Staufen, Germany).

Characterization of microscopic morphology and crystal structure of biochar

The micromorphology of biochar was studied *via* JSM-7610F Field Emission Scanning Electron Microscope (JSM-7610F Schottky Field Emission Scanning Electron Microscope, Tokyo, Japan). The acceleration voltage was 5 KV. The scanning electron microscopy (SEM) images were obtained using an excitation of secondary electrons and backscattered electrons in high vacuum mode. Prior to the observation, biochar samples were sprayed with gold by the JEC-3000FC gold spraying equipment (Auto Fine Coater - JEC-3000FC, Tokyo, Japan).

X-ray diffractometry (XRD) was used to measure the graphitization degree of biochar samples *via* a D2 Phaser diffractometer (BRUKER X-RAY Diffraction D2 Phaser, Karlsruhe, Germany). The experimental conditions of X-ray diffraction were as follows: initial angle was 10°, end angle was 90°, and the time of each step was 0.1 s.

The functional groups present on the surface of the biochar were detected by FTIR using a spectrophotometer (PerkinElmer SPECTRUM 100, Waltham, America) employing the KBr pressing method. The infrared spectrometer was used to measure the range of 4000 to 500 cm^{-1}.

Analysis of adsorption characteristics of biochar

The iodine adsorption value (IAV) of biochar was tested to study its adsorption characteristics and analyzed the degree of pore development according to Chinese National Standard GB/T 12496.8 (2015).

The N_2 isothermal curves, total pore volume, specific surface area, and pore size distribution of the biochar were determined by a fully automated specific surface area porosity analyzer (Autosorb IQ, Boynton Beach, America). The specific surface area of the samples was calculated using the Multi-Point BET method, and the pore size distribution of the biochar was obtained using the DFT method and the BJH method.

RESULTS AND DISCUSSION

Feedstock Properties and Composition

To analyze the properties of pruning wastes as the feedstock for biochar production, ultimate, proximate, chemical composition analysis, and the HHV were conducted and discussed as follows.

The ultimate analysis of feedstock is recorded in Table 1. The elemental content of the wastes of fruit tree pruning varied considerably among tree species. Most of the feedstock is composed of approximately 50% carbon, 6% hydrogen, 0.3 to 0.7% nitrogen, and 40 to 44% oxygen, which is similar to the elemental composition of the pruned fruit tree branch in existing reports (Yu *et al*. 2020). Fruitwood has a higher carbon content than crop straws (around 40%) (Zhao *et al*. 2023), which means that it has a higher calorific value and the potential to produce solid pellet fuels. The low nitrogen of the feedstocks means that virtually no environmentally harmful nitrogen oxides are released during combustion or decomposition.

Table 1. Ultimate Analysis (wt%, Air Dry Basis) of Feedstocks

Tree Species	C (%)	H (%)	O (%)	N (%)
AT	51.98	5.95	42.07	0.29
APT	50.24	5.85	43.91	0.39
WT	51.67	5.83	42.50	0.65
CT	53.82	6.00	40.18	0.44
PT	51.89	6.01	42.10	0.32
MAT-LB	51.56	5.99	42.45	0.31
MAT-MB	52.10	6.02	41.88	0.34
MPT-LB	51.23	5.94	42.83	0.37
MPT-MB	50.96	5.91	43.13	0.32

The results of the proximate analysis and the HHV of fruit tree pruning wastes are recorded in Table 2. The proximate analysis of feedstocks revealed that the volatile content was the highest at 70 to 80%, followed by fixed carbon at around 20%, with ash being the lowest. The calorific value of fruit tree branches was found to range from 17.9 to 19.9 MJ/kg, which is similar to the value of 18.9 MJ/kg reported in previous literature (Bilandzija *et al*. 2012). Compared to crop straws, fruit wood contains lower ash content (Zhai *et al*. 2022), but has higher fixed carbon, making it an ideal material for carbonization. It is worth mentioning that the ash content of chestnut wood pruning wastes was as high as 6.8%, which might be related to the age and high bark content of the tree. In both MAT and MPT tree species, the main branch contained a higher fixed carbon and lower ash content compared to the respective lateral branches, which might be associated with the longer development and greater lignification of the main branches. Fixed carbon, composed chiefly of carbon elements, is the primary substance responsible for heat production during biomass combustion, while ash does not contribute to the heat generation process. Therefore, the calorific value is positively correlated with the fixed carbon content and negatively correlated with ash content, just as APT has the highest fixed carbon content and calorific value of 19.9 MJ/kg. It is worth noticing that the content of each component in the proximate analysis and the HHV is strongly impacted by the plant species and sampling parts (Ślipek *et al*. 2022).

Table 2. Proximate Analysis (wt%, Air Dry Basis) and the Higher Heating Value (MJ/kg) of Feedstocks

Tree Species	Volatile	Fixed Carbon	Ash	Moisture	HHV (MJ/kg)
AT	79.1	17.3	1.0	2.6	19.1
APT	76.4	20.5	1.3	1.8	19.9
WT	73.9	19.8	3.5	2.8	18.1
CT	70.9	19.6	6.8	2.7	17.9
PT	77.4	19.2	0.8	2.6	19.3
MAT-LB	75.4	18.9	2.8	2.9	18.5
MAT-MB	75.3	19.4	2.1	3.2	18.8
MPT-LB	79.3	17.1	1.2	2.4	18.8
MPT-MB	77.2	19.7	0.5	2.6	19.3

The chemical composition of the raw materials analyzed is recorded in Table 3. Pruning wastes of fruit trees are principally composed of carbohydrates (cellulose and hemicellulose, accounting for 70 to 80%), lignin (about 20 to 30%), and extractives (2 to 8%). For the identical tree species, the holocellulose content of lateral branches was higher than that of the main branches, while the lignin content showed the opposite tendency. This may be because of the shorter growth cycle of lateral branches and the lower degree of lignification, which in turn leads to lower lignin content in lateral branches.

Table 3. Chemical Composition Analysis (wt%) of Feedstocks

Tree Species	Cellulose	Holocellulose	Lignin	Extract
AT	37.43	73.01	22.36	5.51
APT	30.17	72.77	25.35	7.71
WT	34.30	71.68	25.65	3.65
CT	26.55	70.14	23.52	6.75
PT	33.97	73.60	25.40	5.31
MAT-LB	31.46	77.84	19.22	3.50
MAT-MB	32.38	70.82	26.15	2.80
MPT-LB	38.61	77.40	22.08	4.82
MPT-MB	37.55	73.40	26.12	4.85

Yield and Energy Consumption of Pyrolysis Products

The distribution of pyrolysis products from fruit tree pruning wastes, the amount of carbon sequestration of biochar, and the electricity consumption during the pyrolysis process are recorded in Fig. 2.

The biomass type and pyrolysis temperature had an important effect on the yield of biochar, wood vinegar, and non-condensable gas (Ortiz *et al*. 2020). When diverse types of feedstocks were pyrolyzed at 500 °C (Fig. 2a), the highest yields of wood vinegar were in the range of 40 to 50%, succeeded by biochar, which accounted for approximately 1/3 of the entire product. The lowest yield was non-condensable gas, approximately 20%.

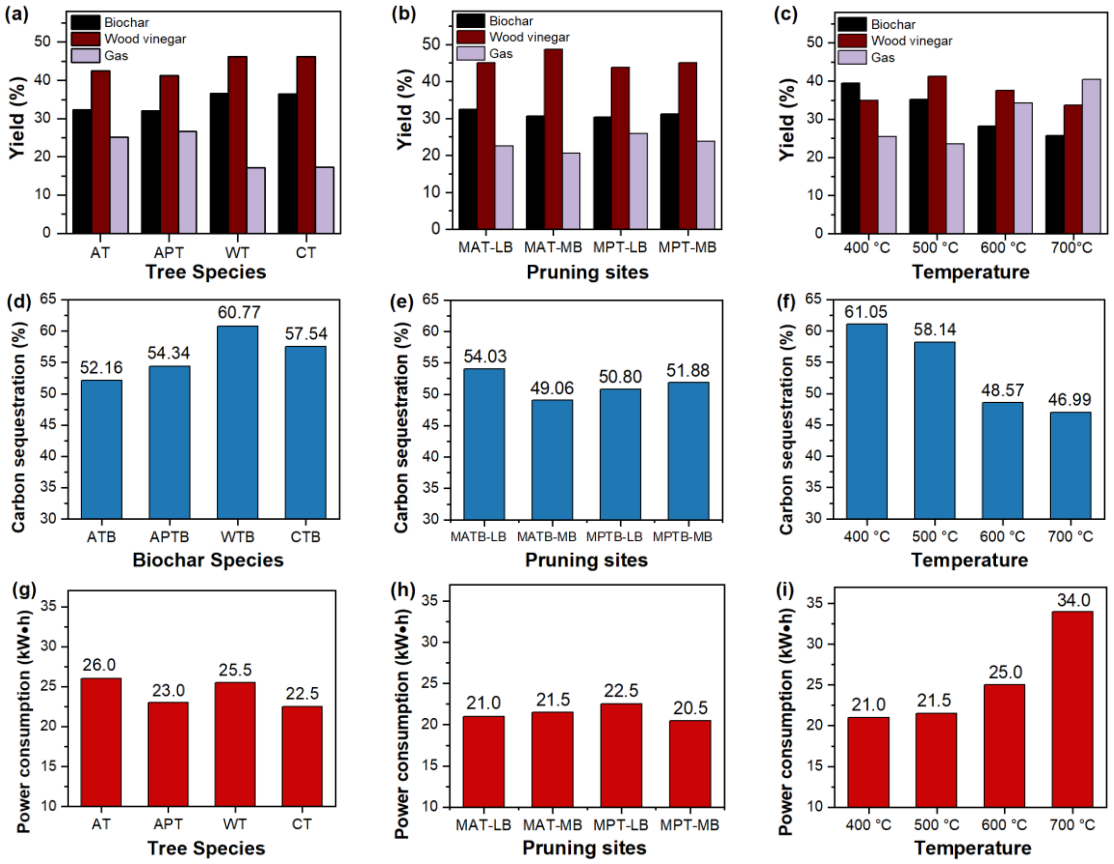

Fig. 2. Distribution of pyrolysis products of fruit wood, carbon sequestration of biochar, and electricity consumption: (a) Yield of pyrolysis products from different tree species; (b) Yield of pyrolysis products from different pruning sites of peach wood; (c) Yield of peach tree pyrolysis products at different temperatures; (d) Carbon sequestered amount of biochar obtained from different tree species; (e) Carbon sequestration amount of biochar obtained from different pruning sites; (f) Carbon sequestration amount biochar obtained from peach wood at different temperatures; (g) Pyrolysis energy consumption of different tree species; (h) Pyrolysis energy consumption of different pruning sites; (i) Pyrolysis energy consumption of peach wood at different temperatures

It is worth mentioning that for different feedstocks under the same experimental conditions, a higher lignin content resulted in a higher biochar yield, which was the case of walnut trees with a maximum lignin content of 25.6% and the highest biochar yield of 36.5%. This was consistent with previous studies that found that lignin contributed most to the formation of biochar (Babinszki *et al*. 2021). As shown in Fig. 2 (b), the distribution of pyrolysis products of the main and lateral branches of mountain peach (mountain apricot) was not apparent, indicating that the effect of biomass species may be more relevant than that of biomass pruning sites in the pyrolysis. When pyrolysis temperature increased (Fig. 2c), biochar yield noticeably decreased, the wood vinegar yield showed a trend of first increasing and then decreasing, reaching a maximum at 500 °C, and the gas yield increased overall. The biochar yield decreased from 35.8% at 400 °C to 24.3% at 700 °C, and the lower biochar yield at higher temperatures was induced by more complete pyrolysis of the feedstocks. Higher temperatures supply more energy for the biomass to break bonds between chemical components, thereby facilitating secondary cracking of hydrocarbons, generating and releasing volatiles, resulting in less biochar but improving its quality and

economic value (Zhang *et al*. 2020). The wood vinegar yield was highest at 500 °C, reaching 46.25%, which was presumably attributable to the primary reaction of the feedstock. When the temperature was elevated from 500 to 700 °C, the wood vinegar yield decreased 7.5%, while the gas yield increased 17%, which may be due to a secondary reaction of the molecules in the wood vinegar (Kaur *et al*. 2023).

When considering the carbon content analysis of feedstock and biochar in Table 1 and Table 3, the biochar captured approximately 44 to 55% of carbon elements present in feedstocks, as illustrated in Fig. 2 (d) through (f). The data presented in Fig. 2 (f) indicates that as the temperature increased, the amount of carbon sequestered by the biochar decreased, which could be because high temperatures cause unstable carbon-containing substances to undergo continuous reactions and be released as gases. Therefore, biochar remains a highly stable substance, which persisted in nature for hundreds of years or even longer, effectively reducing greenhouse gas emissions compared to feedstocks. Studies have demonstrated that if wolfberry branches in Qinghai Province were returned to the soil *via* biochar, 34.42×10^3 tons of carbon element could be sequestered and 68.56×10^3 tons of carbon emissions could be decreased annually from combustion in the atmosphere (Yu *et al*. 2022a). Therefore, the pyrolysis of biomass to manufacture biochar is becoming one of the sustainable solutions for carbon sequestration, lowering greenhouse gas emissions, and combating climate change (Kumar *et al*. 2023).

Electricity was used as the power source for the pyrolysis equipment in this study. In each experiment, 4 kg of feedstocks were pyrolyzed, and electricity consumption was recorded to investigate the effect of species, pyrolysis temperature, and pruning sites on the pyrolysis process, to investigate the economics of this method of biochar production and to optimize the charring process. It has been observed that at a pyrolysis temperature of 500 °C (Fig. 2 (g) through (h)), the energy consumption varies depending on the tree species. Energy consumption was within the range of 20 to 28 kW•h, which may be associated with chemical fraction content of the feedstock. A positive correlation between energy consumption and cellulose content of the feedstock was observed when considering the results in Table 3. Previous studies have shown that the pyrolysis of cellulose exhibited differently from hemicellulose and lignin from the point of energy consumption. The former was endothermic, while that of the latter was exothermic (Yang *et al*. 2007). Furthermore, it should be noted that the activation energy required for the pyrolysis stage of cellulose is higher than that for hemicellulose and lignin (Yeo *et al*. 2019). When pyrolysis of peach wood occurred, biochar obtained at a higher temperature had greater economic value, although the power consumption climbed from 21 kW•h at 400 °C to 34 kW•h at 700 °C, as shown in Fig. 2 (i). This might be because more additional heat was required when the charring furnace reached the targeted temperatures, and the corresponding current intensity would be higher. A forthcoming study will consider the full utilization of the pyrolysis gas to provide power for the pyrolysis of the feedstock, thereby reducing electricity consumption. Furthermore, when different sites of identical tree species were pyrolyzed, the energy consumption of the lateral branches was slightly higher compared to that of the main branches. This was probably because for the identical mass of material, there were more side branches and more gaps between them, so the heat transfer route was relatively longer, which tended to cause more heat loss in the process and thus more power consumption. Overall, these results suggest that the energy consumption during pyrolysis is influenced by various factors, including species, temperature, and pruning location.

Ultimate and Proximate Composition of Fruitwood Biochar

To analyze the properties of pruning waste as the feedstock for biochar production, ultimate, proximate, chemical composition analysis, and the higher heating value were conducted and discussed as follows.

The ultimate analysis of biochar is presented in Table 4. When compared to the elemental content of feedstocks, biochar exhibited a substantial increase in carbon and nitrogen content, while hydrogen and oxygen content demonstrated a decreasing tendency, notably in high-temperature peach wood biochar. The increase in carbon content may be ascribed to the higher degree of carbonization of biomass at elevated temperatures. Additionally, there is a positive correlation between the nitrogen element in biochar and that in the raw material, which is predominantly present in protein and inorganic forms. During the pyrolysis process, these forms are transformed into more stable structures, such as pyrrole-N and graphite-N, thus enhancing the stability of the subsequent biochar (Xu *et al*. 2021). Meanwhile, the decrease in oxygen and hydrogen content could be explained by the cracking of chemical bonds with weak bond energy in biochar at higher temperatures, leading to dehydration and depolymerization reactions. Furthermore, the O/C and H/C ratio in peach wood biochar decreases as the temperature rises (Novak *et al*. 2009), which is an indicator of biochar stability. A lower ratio value indicates that biochar remains to aromatize and carbonize, resulting in higher stable carbon content (Wei *et al*. 2022). Therefore, biochar manufactured at higher temperatures may be relatively higher quality and be more suitable for material applications. These findings have profound implications for the production and utilization of biochar, especially in the context of soil amendment, heavy metal adsorption, and carbon sequestration strategies (Liao *et al*. 2023).

Table 4. The Ultimate Analysis (wt%, Air Dry Basis) of Biochar

Biochar Species	C (%)	H (%)	O (%)	N (%)	H/C	O/C
ATB	82.13	2.68	14.78	0.41	0.0326	0.180
APTB	82.81	2.57	14.06	0.56	0.0310	0.170
WTB	83.09	2.55	13.48	0.88	0.0307	0.162
CTB	82.98	2.54	13.99	0.49	0.0306	0.169
MATB-LB	83.79	2.63	13.24	0.34	0.0314	0.158
MATB-MB	82.09	2.62	14.87	0.42	0.0319	0.181
MPTB-LB	83.47	2.50	13.28	0.75	0.0300	0.159
MPTB-MB	84.17	2.76	12.37	0.70	0.0328	0.147
PTB-400 °C	78.63	3.75	17.09	0.53	0.0477	0.217
PTB-500 °C	83.66	3.02	12.62	0.70	0.0361	0.151
PTB-600 °C	88.28	2.31	8.70	0.71	0.0262	0.099
PTB-700 °C	92.60	1.10	5.57	0.73	0.0119	0.060

Proximate analysis and calorific value of biochar are shown in Table 5, the most abundant component in biochar was fixed carbon, making up around 70 to 80% of its composition. In contrast, volatile content accounted for roughly 20%. Moreover, the HHV of biochar produced at 500 °C was observed to increase almost 50% compared to the feedstocks, reaching 28 to 32 MJ/kg. This value is parallel to, or slightly higher than, the calorific value of standard coal. This rise in HHV was ascribed to the considerable increase in carbon element and fixed carbon content. As the temperature gradually increased from 400 to 700 °C, the volatile content of peach wood biochar underwent a remarkable

reduction, dropping from 30.4% to 5.6%. In contrast, the fixed carbon and ash content increased from 64.1% and 3.2% to 87.1% and 5.2%, respectively. In addition, the HHV of biochar also rose from 29.2 to 31.6 MJ/kg. A possible explanation for this phenomenon is that the unpredictable and low-boiling components in biochar continue to react and discharge volatile substances, leading to the formation of biochar with higher carbon content. This conclusion is consistent with previous experimental results (Kazimierski *et al*. 2021).

Table 5. Proximate Analysis (wt%, Air Dry Basis) and the HHV (MJ/kg) of Biochar

Biochar Species	Volatile	Fixed Carbon	Ash	Moisture	HHV (MJ/kg)
ATB	19.70	74.60	3.10	2.60	30.2
APTB	19.50	74.30	3.40	2.80	29.9
WTB	18.50	73.20	5.00	3.30	28.4
CTB	21.90	71.00	4.70	2.40	28.7
MATB-LB	20.10	70.40	7.30	2.20	28.2
MATB-MB	20.70	69.40	7.80	2.10	28.00
MPTB-LB	17.20	76.30	3.90	2.60	30.40
MPTB-MB	17.60	76.20	4.20	2.00	30.50
PTB-400 °C	30.40	64.10	3.20	2.30	29.20
PTB-500 °C	18.10	76.00	3.60	2.30	30.80
PTB-600 °C	10.40	82.90	4.30	2.40	31.60
PTB-700 °C	5.60	87.10	5.20	2.10	31.30

Micromorphology and Crystalline Structure Analysis of Fruitwood Biochar

The biochar samples obtained from various tree species at 500 °C are depicted in the SEM images in Fig. 3. The biochar exhibited a well-defined porous structure with a distinct regularity. At smaller magnifications (100 μm), the biochar pores derived from walnut branches were observed to be arranged radially in the direction of the wood rays. However, the pore structure of different biochar types exhibited some flocculation when viewed at higher magnifications, which is believed to be caused by incomplete release of volatile components during pyrolysis and subsequent re-condensation of volatiles on the biochar surface during cooling. The good pore structure could promote heat transfer within the feedstock, thereby expediting the pyrolysis process. Simultaneously, the release of water vapor, condensable volatiles, and gases in biomass also had positive effects on the formation of pore structures.

Figure 4 displays the SEM images of peach wood biochar obtained at different pyrolysis temperatures (400, 500, 600, and 700 °C). With an increase in pyrolysis temperature, the number of pores in the biochar increased, along with an expansion in pore size and a thinning of the pore walls of the tubular structure. The changes in the pore structure of the biochar could be ascribed to the formation of air bubbles, while the release of volatile gases at higher temperatures may have acted as pore openers (Mu *et al*. 2023). In particular, at 700 °C the pore structure was smoother and there was nearly no matter produced by condensation of volatile fractions, indicating that volatile gases were released

thoroughly. Thus, the biochar prepared at high temperatures had a rich pore structure compared to low temperatures, which might be attributed to the distinct decomposition temperatures of the various components (cellulose, hemicellulose, lignin, and inorganic minerals) during the pyrolysis procedure. The SEM images of biochar from different parts of the MAT (MPT) were broadly analogous and were therefore not described in detail.

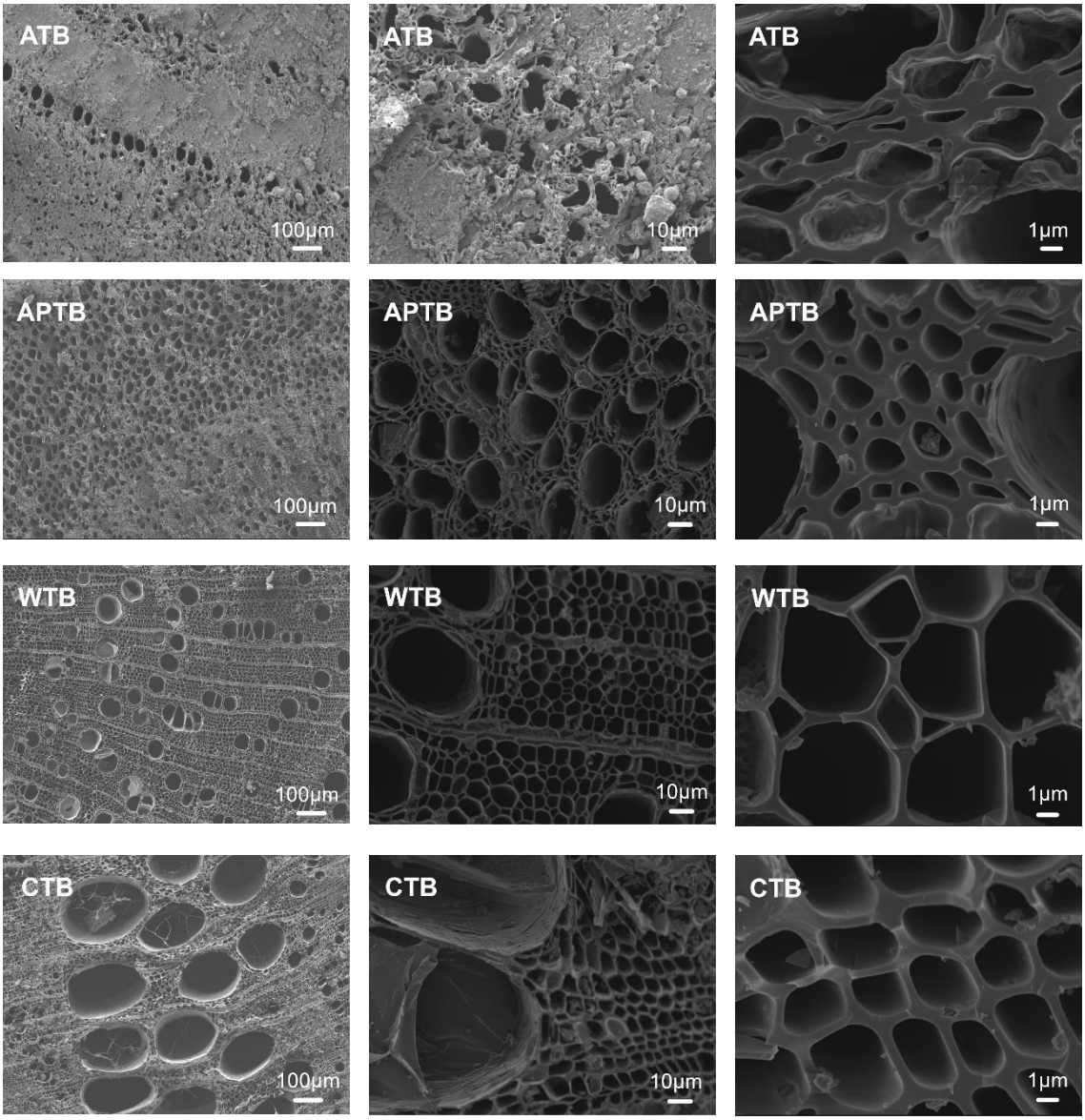

Fig. 3. SEM images of biochar from different tree species; First column (100×), second column (500×), and third column (3000×)

X-ray diffraction is one of the most important means to analyze the crystal structure changes of biochar. The XRD spectra of different types of biochar are shown in Fig. 5. For biochar from different species (Fig. 5a) and pruning sites (Fig. 5b), the positions of the diffraction peaks were consistent, while the intensities varied. The characteristic diffraction peaks around 29.2° and 40° were induced by the presence of mineral crystals in biochar, predominantly including potassium salts, calcium salts, and SiO_2.

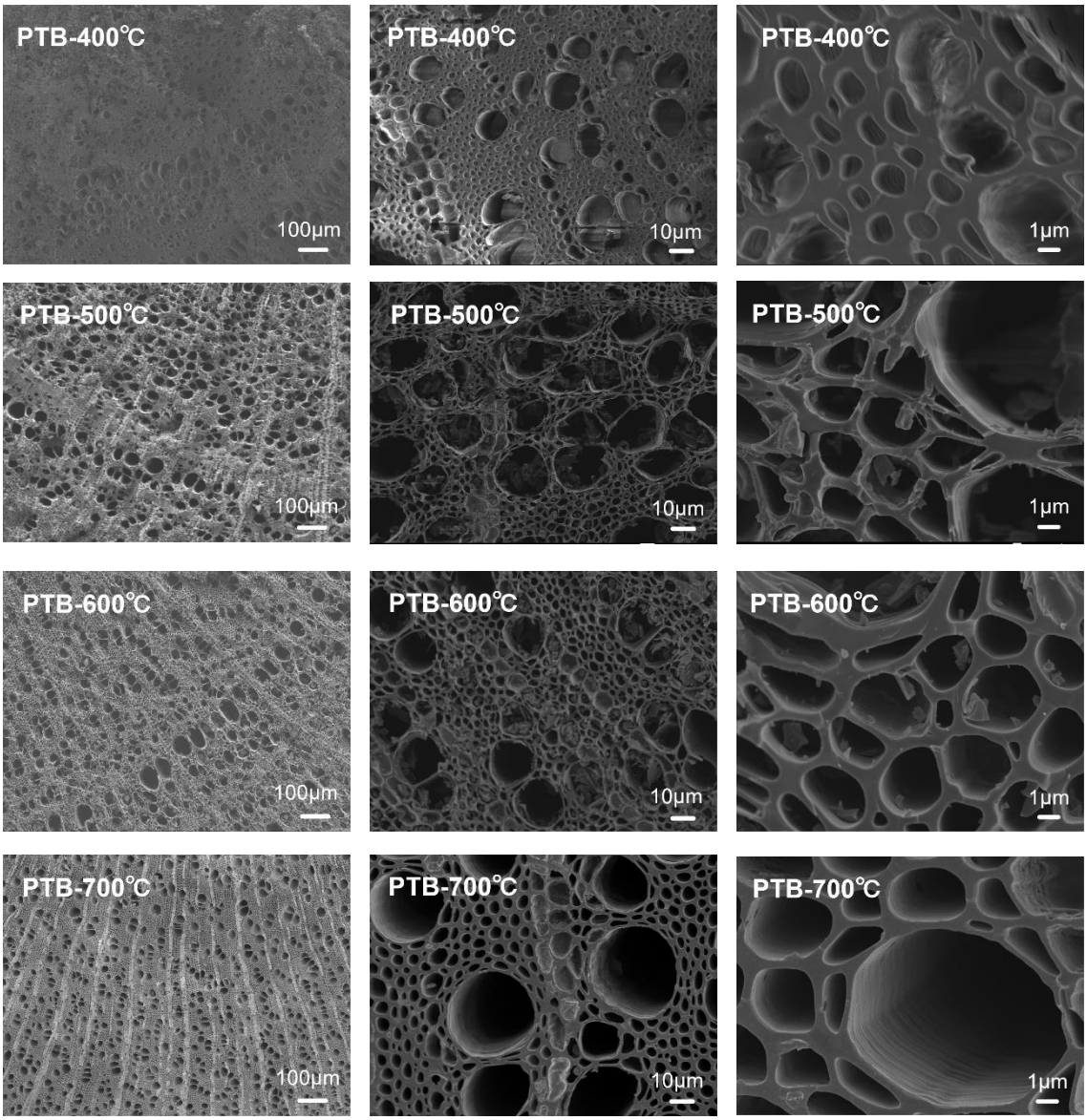

Fig. 4. SEM of peach biochar at different pyrolysis temperatures; First column (100×), second column (500×), and third column (3000×)

Additionally, a positive correlation was observed between the ash content and the diffraction peak intensity at 29.2° and 40° in biochar industrial analysis. Specifically, a higher ash content resulted in a higher diffraction peak intensity. This comparison among biochar highlighted the importance of ash content in determining the diffraction peak intensity. The characteristic diffraction peaks at approximately 23° and 43° correspond to the (002) and (100) crystal faces of the graphite crystal, respectively. The peak (002) represents the reflection of the graphene layer, while the peak (100) represents the reflection of the aromatic ring structure within the graphene layer. With the increase in temperature (Fig. 5c), the diffraction peak of biochar became more apparent at 23°, which was mainly caused by further carbonization. In addition to the change of peak (002), the diffraction peak at 43° (100) also gradually became more obvious (Qin *et al.* 2020). In short, the results of this study indicate that as the pyrolysis temperature rises, the degree of graphitization of biochar also increases gradually.

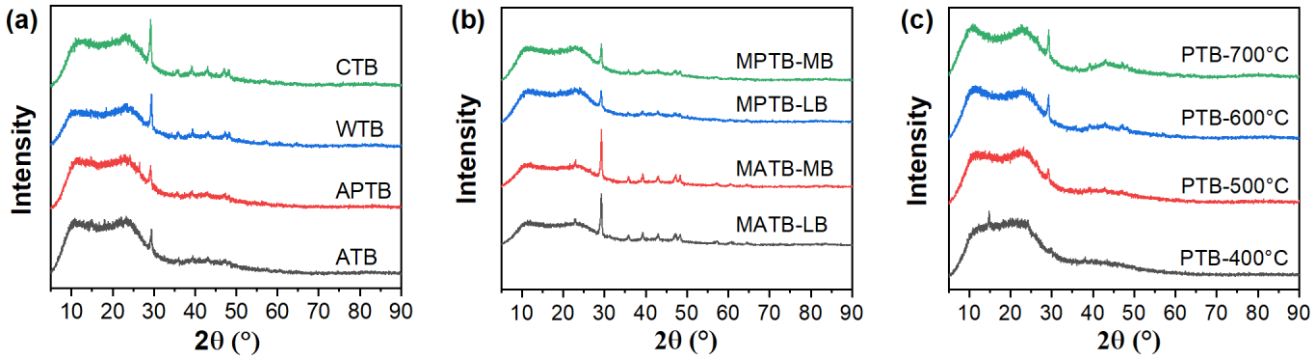

Fig. 5. XRD patterns of biochar produced from different conditions: (a) biochar from different tree species; (b) biochar from different pruning sites; (c) biochar from different temperature

FTIR spectroscopic analysis was used to qualitatively analyze the functional groups present in the materials. Figure 6 exhibits the FTIR spectra of various types of biochar. The absorption peaks close to 3430, 1703, 1600, and 1384 cm^{-1} correspond to the -OH stretching vibration in alcohols or phenols, the C=O stretching vibration in carboxylic acids or carbonyl, the vibration of the benzene ring, and the -CH bending vibration, respectively. The spectral bands located at 3000 to 2850 cm^{-1}, 1300 to 1000 cm^{-1}, and 880 to 680 cm^{-1} can be ascribed to the asymmetric stretching vibration of -CH, the stretching vibration of the C-O-C bond, and the out-of-plane bending vibration of the -CH in aromatic compounds (Lima *et al*. 2021). Thus, it could be found that biochar produced here possessed some typical functional groups, respectively the existence of -OH, alkanes, aromatic rings, carboxylic acids, and ethers. The C-O-C peak area at 1045 cm^{-1} in WTB exceeded that of other biochar (Fig. 6a), which possibly can be attributed to the elevated cellulose content in the feedstock (Fan *et al*. 2021). For biochar at different temperatures (Fig. 6c), the higher the temperature, the lower the peak at 3432 cm^{-1}, indicating that the -OH groups in the biochar decrease with increasing temperature. It also has been observed that the surface functional groups of biochar exhibit a decreasing trend with increasing temperature. Especially at 700 °C, the majority of $-CH_2$ present in the biochar became absent, resulting in the formation of an intricate aromatic structure (Ma *et al*. 2019) that exhibits superior antioxidant and adsorption capacities (Li *et al*. 2017).

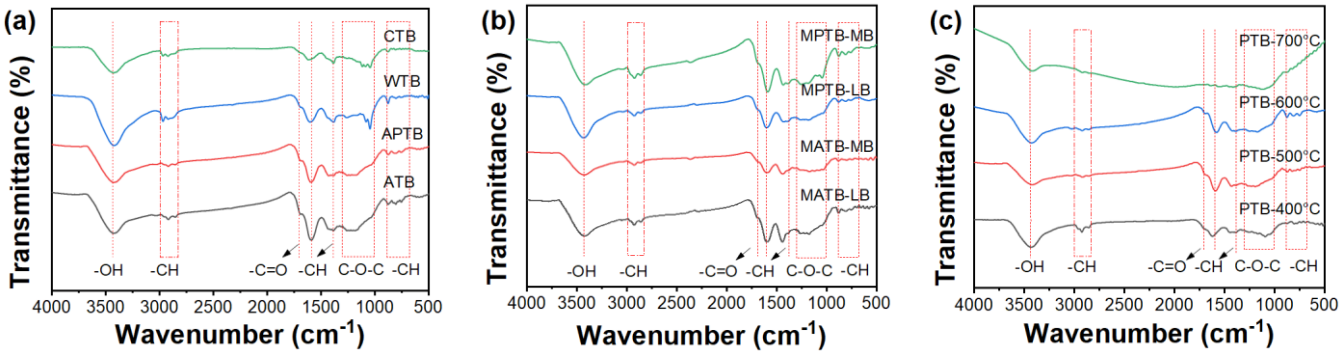

Fig. 6. FTIR spectra of biochar produced from different conditions: (a) biochar from different tree species; (b) biochar from different pruning sites; (c) biochar from different temperature

Adsorption Properties of Fruitwood Biochar

Iodine adsorption is one of the key indicators of the adsorption performance of the char material and is used to evaluate the surface area and degree of micropore development in biochar. The iodine adsorption values of the biochar prepared under different experimental conditions are depicted in Fig. 7. At the same temperature (Fig. 7a), the iodine adsorption values of the biochar varied depending on the species. The lowest was 209 mg/g for ATB and the highest was 248 mg/g for MPB-MB. Compared to the lateral branches, the iodine value of the main branch was higher (Fig. 7b), which may be related to the higher lignification and more developed pore structure of the biochar obtained from the main branch. With increased pyrolysis temperature (Fig. 7c), the iodine value of the biochar expanded from 234 mg/g at 400 °C to 252 mg/g at 700 °C. The high temperature promotes the formation of different pore networks in the biochar, which in turn increases the adsorption capacity of the biochar (Zhao *et al*. 2020). Meanwhile, the content of methylene functional groups on the surface of biochar appeared to decrease at high temperatures, forming an aromatized structure that gave it superior adsorption properties (Selvaraju and Bakar 2017). Therefore, the variation in iodine adsorption value of biochar is mainly due to the difference in texture and surface functional groups. After physical and chemical activation of the produced *Amygdalus communis* shell biochar by Wu *et al.* (2023), the iodine adsorption value of the char material was increased from 424 to 1357 mg/g and the adsorption performance was significantly improved. Therefore, the biochar produced from fruit tree pruning wastes has the potential to produce activated carbon after treatment.

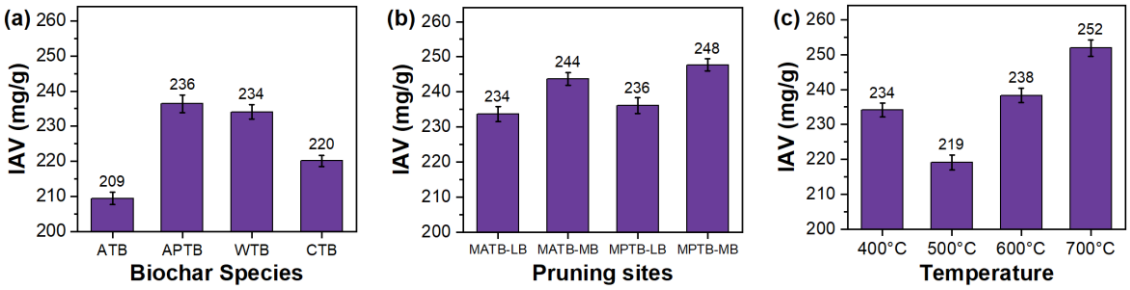

Fig. 7. Iodine adsorption values (IAV) of biochar obtained under different experimental conditions: (a) biochar from different tree species; (b) biochar from different pruning sites; (c) biochar from different temperatures

The adsorption capacity of biochar is largely determined by its specific surface area and pore structure. Figure 8 shows the N_2 adsorption/desorption isotherms (Fig. 8a) and pore size distribution curves (Fig. 8b) of peach wood biochar under optimized conditions at 600 °C. The isotherm of the type I_b (Thommes *et al*. 2015) seemed to be followed for biochar (Fig. 8a), which is the characteristics of micropores (Lima *et al*. 2021). The adsorption and isotherm increased rapidly at low P/P_0, which is mainly dominated by microporous adsorption (Dos *et al*. 2023) and occurs as monomolecular layer adsorption (Pallarés *et al*. 2018). Figure 8 shows that the specific surface area and total pore volume of the biochar were 237 m^2/g and 0.175 cm^3/g, respectively. The pore sizes were distributed within the range of 1.2 to 5.5 nm, with an average pore size of 2.96 nm, which was predominantly microporous and mesoporous. Micropores can increase the total pore volume, and the increase of micropores can provide more adsorption sites, while mesopores can ensure the adsorption rate of biochar.

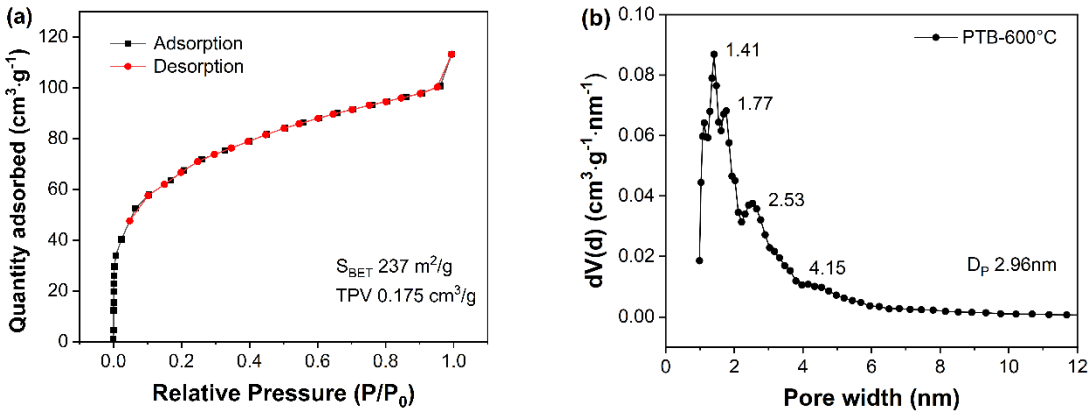

Fig. 8. BET test results of peach wood biochar under optimized conditions (600 °C): (a) N_2 adsorption/desorption isotherms; (b) Pore size distribution curves

CONCLUSIONS

1. Temperature, tree species, and diverse pruning sites of the same tree species have different effects on biochar's energy consumption and physicochemical properties, with temperature being the most dominant factor, followed by tree species, and finally the pruning part of the fruit tree.
2. When the temperature was increased from 400 to 700 °C, the biochar yield decreased from 35.8% to 24.3%, but the properties of biochar were improved, which included a noticeable increase in the carbon element, the fixed carbon content, and the calorific value of biochar, as well as a more developed pore structure.
3. Biochar has a rich variety of surface functional groups, including hydroxyl groups (alcohols, phenols), alkanes, aromatic rings, carboxylic acids, and ethers. The specific surface area, pore volume and average pore size of peach wood biochar produced under optimized conditions at 600 °C were calculated to be 237 m^2/g, 0.175 cm^3/g, and 2.96 nm, respectively. The iodine adsorption values of the biochar could vary based on its surface functional groups and structure properties.
4. Different tree species were pyrolyzed at 500 ℃, wood vinegar yield was highest (40 to 50%), followed by biochar (approximately 33%), and gas (approximately 20%). Biochar can sequester up to 60% of the carbon present in the feedstock, contributing to the reduction of carbon dioxide emissions.

ACKNOWLEDGMENTS

This research was supported by the fund of Hebei Province Central Finance Forest and Grass Science and Technology Promotion Demonstration Project (JI-TG [2022]004), National key research and development program (2022YFD2200904).

CONFLICTS OF INTEREST

The authors declare no conflict of interest.

REFERENCES CITED

Agweh, K., Snowdon, M. R., Mishra, R. K., Chen, G., Vivekanandhan, S., Mohanty, A. K., and Misra, M. (2023). "Production and characterization of waste nutshells derived biocarbon through slow pyrolysis: An investigation on the effects of pyrolysis temperature," *Biomass Convers. Biorefinery* Available Online, 1-15. DOI: 10.1007/s13399-023-03851-4

Aliaño-González, M. J., Gabaston, J., Ortiz-Somovilla, V., and Cantos-Villar, E. (2022). "Wood waste from fruit trees: Biomolecules and their applications in agri-food industry," *Biomolecules* 12(2), article 238. DOI: 10.3390/biom12020238

Babinszki, B., Sebestyén, Z., Jakab, E., Kőhalmi, L., Bozi, J., Várhegyi, G., Wang, L., Skreiberg, Ø., and Czégény, Z. (2021). "Effect of slow pyrolysis conditions on biocarbon yield and properties: Characterization of the volatiles," *Bioresource Technol.* 338, article ID 125567. DOI: 10.1016/j.biortech.2021.125567

Bednik, M. (2022). "Effect of six different feedstocks on biochar's properties and expected stability," *Agronomy* 12(7), article 1525. DOI: 10.3390/agronomy12071525

Bilandzija, N., Voca, N., Kricka, T., Matin, A., and Jurisic, V. (2012). "Energy potential of fruit tree pruned biomass in Croatia," *Span. J. Agric. Res* 10(2), 292-298. DOI: 10.5424/sjar/2012102-126-11

Brand, M. A., and Jacinto, R. C. (2020). "Apple pruning residues: Potential for burning in boiler systems and pellet production," *Renew. Energy* 152, 458-466. DOI: 10.1016/j.renene.2020.01.037

Burachevskaya, M., Minkina, T., Bauer, T., Lobzenko, I., Fedorenko, A., Mazarji, M., Sushkova, S., Mandzhieva, S., Nazarenko, A., Butova, V., *et al*. (2023). "Fabrication of biochar derived from different types of feedstocks as an efficient adsorbent for soil heavy metal removal," *Sci. Rep.* 13(1), 1-14. DOI: 10.1038/s41598-023-27638-9

Chen, D., Li, Y., Cen, K., Luo, M., Li, H., and Lu, B. (2016). "Pyrolysis polygeneration of poplar wood: Effect of heating rate and pyrolysis temperature," *Bioresource Technol.* 218, 780-788. DOI: 1016/j.biortech.2016.07.049

Cheng, S., Liu, Y., Xing, B., Qin, X., Zhang, C., and Xia, H. (2021). "Lead and cadmium clean removal from wastewater by sustainable biochar derived from poplar saw dust," *J. Clean. Prod.* 314, article ID 128074. DOI: 10.1016/j.jclepro.2021.128074

Cheng, S., Meng, M., Xing, B., Shi, C., Nie, Y., Xia, D., Yi, G., Zhang, C., and Xia, H. (2022). "Preparation of valuable pyrolysis products from poplar waste under different temperatures by pyrolysis: Evaluation of pyrolysis products," *Bioresource Technol.* 364, article ID 128011. DOI: 10.1016/j.biortech.2022.128011

Dos Reis, G. S., Bergna, D., Grimm, A., Lima, E. C., Hu, T., Naushad, M., and Lassi, U. (2023). "Preparation of highly porous nitrogen-doped biochar derived from birch tree wastes with superior dye removal performance," *Colloid Surfaces A.* 669, 131493. DOI: 10.1016/j.colsurfa.2023.131493

Fan, M., Li, C., Sun, Y., Zhang, L., Zhang, S., and Hu, X. (2021). "*In situ* characterization of functional groups of biochar in pyrolysis of cellulose," *Sci. Total Environ*. 799, article ID 149354. DOI: 10.1016/j.scitotenv.2021.149354

GB/T 12496.8 (2015). "Test methods of wooden activated carbon—Determination of iodine number," Standardization Administration of China, Beijing, China.
GB/T 2677.10 (1995). "Fibrous material - Determination of holocellulose," Standardization Administration of China, Beijing, China.
GB/T 2677.6 (1994). "Fibrous raw material-Determination of solvent extractives," Standardization Administration of China, Beijing, China.
GB/T 2677.8 (1994). "Fibrous raw material-Determination of acid-insoluble lignin," Standardization Administration of China, Beijing, China.
Januszewicz, K., Kazimierski, P., Klein, M., Kardaś, D., and Łuczak, J. (2020). "Activated carbon produced by pyrolysis of waste wood and straw for potential wastewater adsorption," *Materials* 13(9), article Number 2047. DOI: 10.3390/ma13092047
Kan, T., Strezov, V., and Evans, T. J. (2016). "Lignocellulosic biomass pyrolysis: A review of product properties and effects of pyrolysis parameters," *Renew. Sust. Energ. Rev.* 57, 1126-1140. DOI: 10.1016/j.rser.2015.12.185
Kaur, R., Tarun Kumar, V., Krishna, B. B., and Bhaskar, T. (2023). "Characterization of slow pyrolysis products from three different cashew wastes" *Bioresource Technol.* 376, article ID 128859. DOI: 10.1016/j.biortech.2023.128859
Kazimierski, P., Hercel, P., Suchocki, T., Smoliński, J., Pladzyk, A., Kardaś, D., Łuczak, J., and Januszewicz, K. (2021). "Pyrolysis of pruning residues from various types of orchards and pretreatment for energetic use of biochar," *Materials* 14(11), article 2969. DOI: 10.3390/ma14112969
Kumar Mishra, R., Jaya Prasanna Kumar, D., Narula, A., Minnat Chistie, S., and Ullhas Naik, S. (2023). "Production and beneficial impact of biochar for environmental application: A review on types of feedstocks, chemical compositions, operating parameters, techno-economic study, and life cycle assessment," *Fuel* 343, article ID 127968. DOI: 10.1016/j.fuel.2023.127968
Lee, S. H., Lum, W. C., Boon, J. G., Kristak, L., Antov, P., Pędzik, M., Rogoziński, T., Taghiyari, H. R., Lubis, M. A. R., Fatriasari, W., e*t al*. (2022). "Particleboard from agricultural biomass and recycled wood waste: A review," *J. Mater. Res. Technol-JMRT* 20, 4630-4658. DOI: 10.1016/j.jmrt.2022.08.166
Li, H., Dong, X., Da Silva, E. B., De Oliveira, L. M., Chen, Y., and Ma, L. Q. (2017). "Mechanisms of metal sorption by biochars: Biochar characteristics and modifications," *Chemosphere*. 178, 466-478. DOI: 10.1016/j.chemosphere.2017.03.072
Li, H., Li, Y., Xu, Y., and Lu, X. (2020). "Biochar phosphorus fertilizer effects on soil phosphorus availability," *Chemosphere* 244, article ID 125471. DOI: 10.1016/j.chemosphere.2019.125471
Liao, W., Zhang, X., Ke, S., Shao, J., Yang, H., Zhang, S., and Chen, H. (2023). "The influence of biomass species and pyrolysis temperature on carbon-retention ability and heavy metal adsorption property during biochar aging," *Fuel Process. Technol.* 240, article ID 107580. DOI: 10.1016/j.fuproc.2022.107580
Lima, D. R., Lima, E. C., Thue, P. S., Dias, S. L., Machado, F. M., Seliem, M. K., Sher, F., Dos Reis, G. S., Saeb, M. R., and Rinklebe, J. (2021). "Comparison of acidic leaching using a conventional and ultrasound-assisted method for preparation of magnetic-activated biochar," *J Environ Chem Eng*. 9(5), article ID 105865. DOI: 10.1016/j.jece.2021.105865

Lin, J., Zhang, Q., Xia, H., and Cheng, S. (2022). "Effect of pyrolysis temperature on pyrolysis of pine saw dust and application of bio-char," *Int. J. Environ. Sci. Technol.* 19, 1977-1984. DOI: 10.1007/s13762-021-03159-8

Liu, Z., Jia, M., Li, Q., Lu, S., Zhou, D., Feng, L., Hou, Z., and Yu, J. (2023). "Comparative analysis of the properties of biochars produced from different pecan feedstocks and pyrolysis temperatures," *Ind. Crop. Prod.* 197, article ID 116638. DOI: 10.1016/j.indcrop.2023.116638

Ma, Z., Yang, Y., Wu, Y., Xu, J., Peng, H., Liu, X., Zhang, W., and Wang, S. (2019). "In-depth comparison of the physicochemical characteristics of bio-char derived from biomass pseudo components: Hemicellulose, cellulose, and lignin," *J. Anal. Appl. Pyrol.* 140, 195-204. DOI: 10.1016/j.jaap.2019.03.015

Mu, L., Wang, R., Xie, P., Li, Y., Huang, X., Yin, H., and Dong, M. (2023). "Comparative investigation on the pyrolysis of crop, woody, and herbaceous biomass: Pyrolytic products, structural characteristics, and CO_2 gasification," *Fuel* 335, article ID 126940. DOI: 10.1016/j.fuel.2022.126940

Novak, J. M., Busscher, W. J., Laird, D. L., Ahmedna, M., Watts, D. W., and Niandou, M. A. (2009). "Impact of biochar amendment on fertility of a southeastern coastal plain soil," *Soil Science* 174(2), 105-112. DOI: 10.1097/SS.0b013e3181981d9a

Ortiz, L. R., Torres, E., Zalazar, D., Zhang, H., Rodriguez, R., and Mazza, G. (2020). "Influence of pyrolysis temperature and bio-waste composition on biochar characteristics," *Renew. Energy* 155, 837-847. DOI: 10.1016/j.renene.2020.03.181

Pallarés, J., González-Cencerrado, A., and Arauzo, I. (2018). "Production and characterization of activated carbon from barley straw by physical activation with carbon dioxide and steam," *Biomass Bioenergy*.115, 64-73. DOI: 10.1016/j.biombioe.2018.04.015

Qin, L., Wu, Y., Hou, Z., and Jiang, E. (2020). "Influence of biomass components, temperature and pressure on the pyrolysis behavior and biochar properties of pine nut shells," *Bioresource Technol.* 313, article ID 123682. DOI: 10.1016/j.biortech.2020.123682

Seibold, S., Rammer, W., Hothorn, T., Seidl, R., Ulyshen, M. D., Lorz, J., Cadotte, M. W., Lindenmayer, D. B., Adhikari, Y. P., Aragón, R., *et al*. (2021). "The contribution of insects to global forest deadwood decomposition," *Nature* 597(7874), 77-81. DOI: 10.1038/s41586-021-03740-8

Selvaraju, G., and Bakar, N. K. A. (2017). "Production of a new industrially viable green-activated carbon from *Artocarpus integer* fruit processing waste and evaluation of its chemical, morphological and adsorption properties," *J. Clean Prod*. 141, 989-999. DOI: 10.1016/j.jclepro.2016.09.056

Shaaban, A., Se, S., Dimin, M., Juoi, J. M., Mohd Husin, M. H., and Mitan, N. M. M. (2014). "Influence of heating temperature and holding time on biochars derived from rubber wood sawdust via slow pyrolysis," *J. Anal. Appl. Pyrolysis* 107, 31-39. DOI: 10.1016/j.jaap.2014.01.021

Ślipek, Z., Styks, J., Hebda, T., and Francik, S. (2022). "Physicochemical properties of biochar produced from goldenrod plants," *Materials* 15(7), article 2615. DOI: 10.3390/ma15072615

Soltero, V. M., Román, L., Peralta, M. E., and Chacartegui, R. (2020). "Sustainable biomass pellets using trunk wood from olive groves at the end of their life cycle," *Energy Rep.* 6, 2627-2640. DOI: 10.1016/j.egyr.2020.09.017

Thakkar, J., Kumar, A., Ghatora, S., and Canter, C. (2016). "Energy balance and greenhouse gas emissions from the production and sequestration of charcoal from agricultural residues," *Renew. Energy* 94, 558-567. DOI: 10.1016/j.renene.2016.03.087

Thommes, M., Kaneko, K., Neimark, A., Olivier, J., Rodriguez-Reinoso, F., Rouquerol, J., and Sing, K. (2015). "Physisorption of gases, with special reference to the evaluation of surface area and pore size distribution (IUPAC Technical Report)," *Pure and Appl. Chem*. 87(9-10), 1051-1069. DOI: 10.1515/pac-2014-1117

Wei, M., Marrakchi, F., Yuan, C., Cheng, X., Jiang, D., Zafar, F. F., Fu, Y., and Wang, S. (2022). "Adsorption modeling, thermodynamics, and DFT simulation of tetracycline onto mesoporous and high-surface-area NaOH-activated macroalgae carbon," *J. Hazard. Mater* 425, article ID 127887. DOI: 10.1016/j.jhazmat.2021.127887

Wu, H., Dong, Z., Sun, J., and Ding, K. (2023). "Boosting the adsorption capacity of activated carbon prepared from *Amygdalus communis* shells using physicochemical co-activation method," *Biomass Convers. Biorefinery*. Available Online, 1-11. DOI: 10.1007/s13399-023-04093-0

Xu, S., Chen, J., Peng, H., Leng, S., Li, H., Qu, W., Hu, Y., Li, H., Jiang, S., Zhou, W., and Leng, L. (2021). "Effect of biomass type and pyrolysis temperature on nitrogen in biochar, and the comparison with hydrochar," *Fuel* 291, article ID 120128. DOI: 10.1016/j.fuel.2021.120128

Yang, X., Kang, K., Qiu, L., Zhao, L., and Sun, R. (2020). "Effects of carbonization conditions on the yield and fixed carbon content of biochar from pruned apple tree branches," *Renew. Energy* 146, 1691-1699. DOI: 10.1016/j.renene.2019.07.148

Yang, H., Yan, R., Chen, H., Lee, D. H., and Zheng, C. (2007). "Characteristics of hemicellulose, cellulose and lignin pyrolysis," *Fuel* 86(12-13). 1781-1788. DOI: 10.1016/j.fuel.2006.12.013

Yeo, J. Y., Chin, B. L. F., Tan, J. K., and Loh, Y. S. (2019). "Comparative studies on the pyrolysis of cellulose, hemicellulose, and lignin based on combined kinetics," *J. Energy Inst*. 92(1), 27-37. DOI: 10.1016/j.joei.2017.12.003

Yu, J., Song, M., and Li, Z. (2022a). "Optimization of biochar preparation process and carbon sequestration effect of pruned wolfberry branches," *Green Process. Synth.* 11(1), 423-434. DOI: 10.1515/gps-2022-0044

Yu, S., Wang, L., Li, Q., Zhang, Y., and Zhou, H. (2022b). "Sustainable carbon materials from the pyrolysis of lignocellulosic biomass," *Mater. Today Sustain.* 19, article ID 100209. DOI: 10.1016/j.mtsust.2022.100209

Yu, T., Abudukeranmu, A., Anniwaer, A., Situmorang, Y. A., Yoshida, A., Hao, X., Kasai, Y., Abudula, A., and Guan, G. (2020). "Steam gasification of biochars derived from pruned apple branch with various pyrolysis temperatures," *Int. J. Hydrog. Energy* 45(36), 18321-18330. DOI: 10.1016/j.ijhydene.2019.02.226

Zhai, P., Zhao, Y., Yang, S., Jin, X., Liang, Z., Yuan, H., Li, C. Z., and Li, C. J. (2022). "Comparison of yield and physicochemical characteristics of tropical crop residue biochar under different pyrolysis temperatures," *Biomass Convers. Biorefinery* Available Online, 1-13. DOI: 10.1007/s13399-022-03058-z

Zhang, X., Zhang, P., Yuan, X., Li, Y., and Han, L. (2020). "Effect of pyrolysis temperature and correlation analysis on the yield and physicochemical properties of crop residue biochar," *Bioresource Technol.* 296, article ID 122318. DOI: 10.1016/j.biortech.2019.122318

Zhao, C., Liu, X., Chen, A., Chen, J., Lv, W., and Liu, X. (2020). "Characteristics evaluation of bio-char produced by pyrolysis from waste hazelnut shell at various temperatures," *Energy Sources Part A – Recovery Util. Environ. Eff* Available Online, 1-11. DOI: 10.1080/15567036.2020.1754530

Zhao, F., Wang, F., Zhang, F., Liu, S., Duan, P., and Yan, W. (2023). "Catalytic hydropyrolysis of crop straws with different biochemical composition," *Int. J. Hydrog. Energy* 48(19), 6927-6936. DOI: 10.1016/j.ijhydene.2022.03.047

Article submitted: August 26, 2023; Peer review completed: September 30, 2023; Revised version received and accepted: October 21, 2023; Published: October 30, 2023.
DOI: 10.15376/biores.18.4.8536-8556